Sub-Photospheric Emission from Relativistic Radiation Mediated Shocks in GRBs

Omer Bromberg[1], Ziv Mikolitzky[2] & Amir Levinson[2]

[1] Racah Institute of Physics, The Hebrew University, 91904 Jerusalem, Israel

[2] The Raymond and Berverly Sackler School of Physics and Astronomy, Tel Aviv University, 69978 Tel Aviv, Israel

Abstract

It is proposed that the prompt emission observed in bursts that exhibit a thermal component originates from relativistic radiation mediated shocks that form below the photosphere of the GRB outflow. It is argue that such shocks are expected to form in luminous bursts via collisions of shells that propagate with moderate Lorentz factors $\Gamma \lesssim 500$. Faster shells will collide above the photosphere to form collisionless shocks. We demonstrate that in events like GRB 090902B a substantial fraction of the explosion energy is dissipated below the photosphere, in a region of moderate optical depth $\tau \lesssim 300$, whereas in GRB 080916C the major fraction of the energy dissipates above the photosphere. We show that under conditions anticipated in many GRBs, such relativistic radiation mediated shocks convect enough radiation upstream to render photon production in the shock transition negligible, unlike the case of shock breakout in supernovae. The resulting spectrum, as measured in the shock frame, has a relatively low thermal peak, followed by a broad, nonthermal component extending up to the KN limit.

1 Introduction

According to the standard view, the prompt GRB emission is produced behind internal shocks that form in the coasting region of a baryon loaded fireball (e.g. Levinson & Eichler, 1993; Rees & Meszaros, 1994; Sari & Piran,

1997). The emission mechanism commonly invoked is synchrotron cooling of relativistic electrons that are accelerated at the shock front, perhaps accompanied by synchrotron-self Compton emission at highest energies. In order to be able to accelerate particles the shocks must be collisionless. As argued below (see also Levinson & Bromberg 2008, hereafter LB08), under the conditions anticipated such shocks can only form in regions where the optical depth for Thomson scattering is smaller than unity, as otherwise the radiation produced in the shock transition and in the immediate downstream mediates the shock via Compton scattering. Thus, an implicit assumption of the standard fireball model is that a significant fraction of the bulk energy dissipates above the photosphere.

The fireball model outlined above was originally motivated by the detection of nonthermal spectra in many GRBs. Despite some difficulties in associating the low energy part of the spectrum with optically thin synchrotron emission (e.g. Crider et al. 1997; Preece et al. 1998), some believed that this model can account for the Band spectrum (Band et al., 1993) inferred in many sources.

The difficulties with the synchrotron model, as well as other considerations (e.g. Eichler & Levinson 2000), have led to the suggestion that photospheric emission may contribute to the prompt GRB spectrum, in addition to the observed non-thermal component (e.g. Mészáros & Rees 2000, Mészáros *et al.* 2002). At the same time, it has been argued that a combination of a thermal and a nonthermal components can fit better the data in quite a number of bursts (e.g. Ryde 2004, 2005, 2006, Pe'er *et al.* 2007, Pe'er 2008). The recent detections of a prominent thermal peaks in several LAT bursts, notably GRB 090902B (Abdo et al., 2009b; Ryde et al., 2010), provide a strong support to this interpretation.

The conditions at the shock formation region depend on the power and Lorentz factor of the outflow and the duty cycle of the central engine. For shells to collide above the photosphere, the Lorentz factor must be large enough. As shown below, in some bursts, e.g., GRB 080916C, internal shocks are expected to form above the photospher, whereas in others, e.g., GRB 090902B, a major fraction of the energy is likely to dissipate below the photosphere, albeit in a region of moderate optical depth. Indeed, the spectrum of GRB 080916C is well fitted by a broken power law (Abdo et al., 2009a), while that of GRB 090902B exhibits a thermal peak (Abdo et al., 2009b; Ryde et al., 2010).

The above considerations motivate detailed investigation of the properties

of shocks that form below the photosphere, in regions where the Thomson optical depth exceeds unity. Preliminary studies indicate that such shocks are mediated by Compton scattering of radiation produced in the shock transition layer or convected by the upstream flow (LB08; Katz et al., 2010; Budnik et al., 2010). The typical width of the shock transition, a few Thomson mean free paths, is much larger than any kinetic scale involved, rendering particle acceleration in such shocks highly unlikely. Thus, the photon spectrum produced in relativistic radiation mediated shocks (RRMS) may be considerably different than that anticipated in collisionless shocks. Moreover, the radiation produced downstream is trapped for times much longer than the shock crossing time, and diffuses out after the shock breaks out of the photosphere and becomes collisionless. Consequently, any rapid fluctuations of the flow parameters will be smeared out, and may not be imprinted in the observed gamma-ray emission.

In this paper we explore the role of RRMS in the prompt phase of GRBs. A qualitative discussion of RMS is given in §2. In §3 we analyze regimes in the parameter space in which overtaking collisions of shells occur below and above the photosphere. In §4 we investigate the properties of RRMS that form during the prompt GRB phase. We show that under conditions anticipated in many GRBs, such relativistic radiation mediated shocks convect enough radiation from the upstream to render photon production in the shock transition negligible, unlike the case of shock breakout in supernovae and hypernovae (e.g., Weaver 1977; Katz et al. 2010). Bulk Comptonization then produces a relatively low thermal peak, followed by a broad, nonthermal component in the immediate downstream. To illustrate some properties of the spectrum we present, in §5, test particle Monte Carlo simulations of bulk Comptonization. The shock structure computed in LB08 is used as input to these simulations. In the regime where photon convection is important the analysis of LB08 is justified, and the shock solutions obtained there present reasonable approximations. We find that a hard tail extending up to the KN limit (roughly $\sim \Gamma m_e c^2$ in the observer frame) is a generic feature of RRMS in GRBs. We conclude in §6.

2 RMS - a qualitative discussion and review of previous work

The structure of non-relativistic RMS was first studied by Pai (1966), Zel'dovich & Raizer (1967) and by Colgate & Chen (1972). These authors assumed that the plasma and the radiation field maintain local thermodynamic equilibrium (LTE) at the shock transition, giving rise to a black body spectrum. Under this assumption the temperature increases monotonically from the upstream to the downstream. Weaver (1976) extended this analysis to include conditions anticipated in supernovae shock breakout, where the upstream is cold and photon poor. He showed that when the shock velocity exceeds ~ 0.03c and the upstream temperature $KT_u \lesssim 1\ n_{b,15}^{1/3}$ eV, where $n_{b,15}$ is the baryons mass in units of 10^{15} gr, the photon production rate is insufficient to sustain a black body distribution within the shock transition. As a consequence, the photons can only maintain Wien equilibrium with the plasma, defined as a Planck spectrum with a non-vanishing chemical potential, and a temperature equal to that of the electrons. Since fewer photons supply the shock pressure, the temperature rises above its value at the far downstream, where thermodynamic equilibrium is re-established. At $\beta_u \sim 0.2$ the peak temperature reaches values of $KT \sim 10$ KeV, approximately two orders of magnitude above the black-body temperature further downstream. At such velocities the photon production rate in the transition region is negligible, and the majority of photons which support the shock are created downstream of the deceleration zone, and diffuse back to the upstream (Katz et al., 2010). Higher upstream velocities lead to increased pair production- and annihilation rates up to a point where the amount of MeV photons begins to affect the flow. In this case, the full KN cross section must be used to correctly solve the shock. RMS in this limit are analyzed by (Budnik et al., 2010).

When the photon-to-electron ratio in the upstream region is high enough, the total production rate of photons in the transition region (due to local emission processes and diffusion from the downstream) is negligible; it may be assumed that the photon number is conserved within the shock. Blandford & Payne (1981a,b; hereafter BP81a,b) investigated such shocks in the limit of non relativistic upstreams and vanishing thermal effects, and obtained a self-consistent solution for the structure of the shock and for the transmitted radiation spectrum. They showed that photons which are advected with the flow across the shock, can diffuse back to the upstream and traverse

the shock once more. In each crossing the photons gain a small amount of energy as a result of the flow compression. Some of these photons are caught in the shock, and by experiencing this process multiple times, undergo a substantial energy buildup, resulting in a power law tail which extends to high energies, similar to first order Fermi acceleration of cosmic rays (for a review see Blandford & Eichler, 1987). The solution provided by BP81b for the transmitted spectrum is valid as long as the average energy gain per scattering due to compressional heating (bulk motion), $\sim \beta^2$, sufficiently exceeds the corresponding energy gain due to thermal Comptonization $\sim \frac{KT_e}{m_e c^2}$. This condition is equivalent to the requirement that the Compton parameter satisfies $y_C \lesssim 1$, and holds for fast, cold flows. BP81b solution was generalized by Lyubarsky & Sunyaev (1982), Riffert (1988) and Becker (1988) to include thermal processes as well.

In the non-relativistic regime, where the upstream velocity $\beta_u \ll 1$ and the temperature across the shock $T \ll m_e c^2/K$, several approximations can be made which greatly reduce the complexity of the solution. Firstly, the Thomson cross section σ_T can be used in the radiation transfer equation, instead of the full KN formula. Secondly, as the radiation field anisotropy in the fluid rest frame is always small, the motion of the photons across the shock can be regarded as a diffusive process. In such process the number of scatterings that a photon undergoes as it passes through the shock deceleration region is $N = (L_s/\lambda_T)^2$, where L_s is the width of the deceleration region and $\lambda_T = (n_e \sigma_T)^{-1}$ is the photon mean free path. If the diffusion time roughly equals to the shock crossing time then $\lambda_T N \simeq L_s/\beta_u$. Consequently $N \simeq \beta_u^{-2}$ and $L_s \simeq (n_e \sigma_T \beta_u)^{-1}$. Finally, to order β_u^2, the radiation field satisfies the equation of state $P_r = U_r/3$, which provides a closure condition for the set of hydrodynamic equations governing the shock structure (e.g. Hsieh & Spiegel, 1976).

When β_u approaches unity the photon distribution function becomes highly anisotropic and the diffusion approximation breaks down. A completely different method of solution is then required. In addition, pair creation inside the shock transition may be important and needs a proper treatment. LB08 computed the structure of the shock transition for various upstream condition, using multiple moments expansion of the transfer equation. They assumed that the photon number is roughly conserved across the shock transition, which is justified when photon advection by the upstream fluid dominates over photon production, and neglected pair creation by nonthermal photons. They found, as expected, that the thickness of the shock is

of the order of a few Thomson lengths. Recently, Budnik et al. (2010) calculated numerically the structure and spectrum of RRMS for sufficiently relativistic, cold upstream. They have shown that the spectrum consists of a thermal peak at $m_e c^2$ roughly, followed by a hard tail that extends up to $\Gamma_u^2 m_e c^2$, as measured in the shock frame. The high temperature in the immediate downstream is a consequence of the paucity of photons advected from the upstream, resulting in intensive pair cascade at the immediate downstream which keeps the temperature at this level. A much lower temperature is anticipated in the RRMS which are expected to form in the photons rich jets of GRBs, as discussed below.

3 Formation of RRMS in GRB outflows

To investigate the conditions under which shells may collide below the photosphere we consider a conical fireball having an isotropic equivalent luminosity L_{iso}. We assume that the fireball is ejected with an initial Lorentz factor $\Gamma_0 \sim 1$ from a compact central engine of radius R_0, and that it carries baryons with an isotropic mass loss rate $\dot{M}_b$. The properties of the fireball, and in particular the location of the photosphere depend of the dimensionless parameter $\eta \equiv \frac{L_{iso}}{\dot{M}_b c^2}$. When $\eta < \eta_c$, where

$$\eta_c = \left(\frac{\sigma_T L_{iso} \Gamma_0}{4\pi R_0 m_b c^3} \right)^{1/4} = 1.8 \times 10^3 L_{52}^{1/4} R_6^{-1/4} \Gamma_0^{1/4}, \qquad (1)$$

the fireball is sufficiently opaque, such that the radiation is trapped during the entire acceleration phase. The major fraction of the explosion energy is then converted into bulk kinetic energy of the baryons, and the fireball reaches a terminal Lorentz factor $\Gamma_\infty \simeq \eta$ at some radius $r_* \simeq \eta R_0/\Gamma_0$, beyond which it continues to coast. The photosphere is located somewhere in the coasting region, at $r_{ph} > r_*$. On the other hand, when $\eta > \eta_c$ the fireball will become transparent already during the acceleration phase, before reaching the coasting radius $r = \eta_c R_0/\Gamma_0$. The Loerentz factor in that case is limited by η_c [1].

[1] If $\eta > \eta_c$ the acceleration continues beyond the photosphere, since the photon flux is high enough to sustain efficient acceleration even though only a fraction of the photons undergo scatterings (see Mészáros & Rees, 2000; Nakar et al., 2005).

The optical depth at a radius r, defined as $\tau(r) = \int_r^\infty \sigma_T n_l \Gamma^{-1} dr$, can be expressed in terms of the fireball parameters as [2]

$$\tau(r) = \frac{\eta_c^4 R_0}{\eta^3 \Gamma_0 r} \begin{cases} \left[3 - 2(\eta_c/\eta)^4\right]^{-1} (\eta R_0/\Gamma_0 r)^2 & \eta_c < \eta, \\ 1 & \eta < \eta_c. \end{cases} \quad (2)$$

The photospheric radius r_{ph} can be found from the condition $\tau(r_{ph}) = 1$, and it is readily seen that for $\eta = \eta_c$ one has $r_{ph} = \eta_c R_0/\Gamma_0 = r_*$.

Suppose now that intermittencies of the central engine lead to ejections of shells that collide at some radius r_d. Let Γ_1 denote the Lorentz factor of a shell ejected at time t_0 and $\Gamma_2 = b\Gamma_1$ the Lorentz factor of a second shell ejected at $t_0 + \delta t$. If $b > 1$ the shells collide at $r_d \simeq 2\Gamma_1^2 c \frac{b^2}{b^2-1}\delta t$. Now, if $\eta < \eta_c$ then the shells collide in the coasting region and we have $\Gamma_1 \simeq \eta$. The optical depth at the radius of collision is obtained from Eq. (2):

$$\tau(r_d) = \frac{\eta_c^4}{2\Gamma_0 \eta^5} \left(\frac{c\delta t}{R_0}\right)^{-1} (1 - b^{-2}), \quad (3)$$

and it is seen that collision will occur below the photosphere, viz., $\tau(r_d) > 1$ if

$$\Gamma_1 < \eta_{ph} \equiv 360 L_{52}^{1/5} R_6^{1/5} (1 - b^{-2})^{1/5} \left(\frac{c\delta t}{R_0}\right)^{-1/5}. \quad (4)$$

As can be seen from Eq. (4) it is easier for internal shocks to form below the photosphere in bursts with high luminosity. Such high luminous bursts with $L_{iso} \sim$ a few 10^{53} ergs/s are detected now by the *Fermi* satellite. These bursts are characterized by an initial prompt phase with a maximal energy $\lesssim 10$ MeV and a peak energy at about 1 MeV, followed by a longer phase characterized by a harder spectrum extending up to 10 GeV and a larger peak energy. The Lorentz factors, inferred from the requirement that the shell should be optically thin for the GeV photons, are usually high with $\Gamma > 500$, but these are model dependent (see e.g. Zou et al., 2011, for lower values). Table 1 shows some relevant values for 3 such bursts, where $\Gamma_{min,1}$ is the minimal estimated Lorentz factor assuming two separate emission zones for the MeV and for the GeV photons (Zou et al., 2011), and $\Gamma_{min,2}$ is the minimal Lorentz factor assuming a single emission zone.

[2] For simplicity we assumed an infinite medium. If the shock forms inside a finite shell, the upper limit of the integration should change to $2r$ (e.g. Shemi & Piran, 1990; Mészáros et al., 1993; Nakar et al., 2005), but that will have only minor effect on our results.

In fig (1) we plot $\tau(r_d)$ as a function of the shell's Lorentz factor, for the 3 bursts shown in table 1. The bold lines depict constant δt, and span a range between R_0/c and a maximal time interval, taken to be the observed variability time by the *Fermi* BGO detector. The colored areas mark the range of Γ and δt relevant for each burst. As can be seen shells with $\Gamma > 700$ collide above the photosphere, resulting in shocks which are most likely collisionless. On the other hand, slower shells ejected over time scales which are closer to the dynamical time scale of the system, collide below the photosphere leading to the formation of RMS. The parameter space explored in fig (1) indicates that in GRB 080916C, the majority of the GRB energy dissipates above the photosphere, therefore a thermal component may be very week or absent. In GRB 090902B, however a major fraction of the energy is likely to dissipate below the photosphere, in a region of moderate optical depth ($\tau < 300$). Indeed a prominent thermal component in the prompt soft phase accompanied by a hard tail was reported in this burst (Abdo et al., 2009b), as expected in a case of RRMS (see §5). In the short GRB 090510, a moderate fraction of the jet energy may dissipate below the photosphere. The interpretation of the soft initial phase in this burst however is not clear and may fit a Band spectrum such as expected from Collisionless shocks, as well as a photospheric emission with a (quasi) thermal component (see e.g. Ackermann et al., 2010; Pelassa & Ohno, 2010).

Note that much longer variability time scale is anticipated in a case where the shock forms below the photosphere, and the downstream radiation is trapped for times much longer than the shock crossing time, and diffuses out after the shock breaks out of the photosphere. Therefore the observed variability timescales do not necessarily reflect the actual time separation between the shells, which may be much shorter. At what depth downstream of the shock equilibrium is established is yet an open issue. Since the enthalpy downstream is dominated by radiation, a full equilibrium is not expected for the moderate optical depths found above (see further discussion in §5). The photons produced by RMS can reach energy of $\gtrsim \Gamma m_e c^2 = 0.25 \left(\frac{\Gamma}{500}\right)$ GeV in the observer frame, which is more then enough to account for the energy range observed during the soft phase.

Table 1 Parameters of Fermi LAT bursts

GRB	T_{90}(s)	E_{iso}(erg)	L_{iso}(erg/s)	δt^*_{var} (ms))	$\Gamma_{min,1}$	$\Gamma_{min,2}$
$080916C$[1]	66	$8.8 \cdot 10^{54}$	$3.3 \cdot 10^{53}$	512	488[2]	890[1]
090510[3]	0.5	$1.1 \cdot 10^{53}$	$2.7 \cdot 10^{53}$	14	324[2]	720[3]
$090902B$[4]	30	$3.63 \cdot 10^{54}$	$2.4 \cdot 10^{53}$	53	253[2]	550[5]

(1) Abdo et al. (2009a); (2) Zou et al. (2011); (3) Ackermann et al. (2010); (4) Abdo et al. (2009b); (5)Ryde et al. (2010)
* The variability is measured with the BGO detector (150 Kev - 40 MeV).

4 Properties of RMS with photon rich upstreams

Consider an infinite plane parallel RMS moving in the x direction. The shock transition is defined within a region bounded by $x_s - L_s$ and x_s, where $\beta = \beta_u$ if $x < x_s - L_s$ and $\beta = \beta_d$ if $x > x_s$. Far from the transition region the photons maintain thermodynamic equilibrium with the plasma, and have a black body distribution with an average energy per photon $\langle h\nu' \rangle_{u(d)} = 3KT'_{u(d)}$. Hereafter primed quantities are measured in the fluid rest frame and unless stated otherwise, unprimed quantities refer to the shock frame. We define the shock upstream to be photon-rich, if the "effective" increase in the photon number when passing through the shock transition is small. The term "effective" is used to indicate that only those photons which significantly contribute to the pressure are accounted for (see similar analysis in Katz et al., 2010, but in a different regime of parameters spance). Taking $T'_s \equiv T'(x_s)$ as the typical temperature at the shock transition[3], photons which are produced with energies $\ll KT'_s$ can also contribute to the radiation pressure, if they can be IC upscattered to energies of $\sim KT'_s$ during the passage through the shock. In non-relativistic RMS, where thermal Comptonization is the dominant heating mechanism, a photon can double its energy after $\sim \frac{m_e c^2}{4KT'_s}$ scatterings. Therefore, the lowest frequency above which the photon energy

[3]In shocks where bulk acceleration is significant, the spectrum is non-thermal; defined as such, this temperature represents the ratio between the radiation pressure and the photon number density. Note that the peak temperature in the shock may be higher than T'_s, yet we find that in the parameter regime relevant here, the difference never exceeds an order of a few.

can significantly increase is set by the condition $\alpha_{ff}\lambda_T \frac{mc^2}{4KT'_s} < 1$, where α_{ff} is the free-free absorption coefficient (e.g. Rybicki & Lightman, 1979), giving $h\nu'_{min} \sim 50\ eV\ n'^{0.5}_{15} \left(\frac{KT'_s}{100eV}\right)^{-5/4}$. Such a photon can reach the peak energy within the shock crossing time if $y_C > ln\left(\frac{KT'_s}{h\nu'_{min}}\right)$ (Weaver, 1976; Katz et al., 2010). If, however, bulk acceleration is the dominant mechanism, $y_C \simeq 1$, and only photons with energies above $h\nu'_{min} \sim KT'_s/2$ can contribute to the pressure. When $\gamma_u \gg 1$ each photon undergoes only a few scatterings, experiencing an energy increase $\lesssim \gamma_u^2$. Therefore $h\nu'_{min} \sim KT'_s/\gamma_u^2$ at this limit.

In addition to the Comptonization processes, emission can also be an important source of photons if the photons production time is shorter than the shock crossing time. Svensson (1984) demonstrated that the two most dominant emission processes in a thermal plasma, when pair density is negligible, are e-p Bremsstrahlung and double Compton (DC). The effective photon generation rate by Maxwellian e-p Bremsstrahlung emission is:

$$\dot{n}'_{ff} = \sqrt{\frac{32\pi}{3}} \left(\frac{T'}{m_e c^2}\right)^{-1/2} (n'_l \sigma_T c) n'_b \alpha \Lambda_{ff}, \tag{5}$$

where $\Lambda_{ff} \equiv \left(-\mathrm{Ei}(\frac{h\nu'_{min}}{m_e c^2})\right) \cdot g_{ff}$, $\mathrm{Ei}(x)$ is the exponential integral of x, and g_{ff} is the Gaunt factor (e.g. Rybicki & Lightman, 1979). For the above estimations of $h\nu'_{min}$ it is safe to assume that $\Lambda_{ff} \lesssim 10$ for most upstream conditions. Here and for the rest of the paper, electrons and protons are assumed to have a Maxwellian distribution. This assumption relies on the fact that the relaxation time of an electron in restoring a Maxwellian distribution with temperature T_e is of the order of $t_e \sim (n_l \sigma_T c\ \mathrm{ln}\lambda)^{-1} (\mathrm{kT_e/m_e c^2})^{3/2}$, where λ is the Coulomb logarithm (see Spitzer, 1978, BP81a). For electrons with subrelativistic temperatures this time is much shorter than the average time between scatterings, $t_c \sim (n_l \sigma_T c)^{-1}$. Svensson (1984) calculated the production rate of photons by DC emission in the limit of soft photons ($h\nu' \ll \min(m_e c^2, KT')$), having a Wien distribution and maintaining thermal equilibrium with electrons. He showed this rate to be

$$\dot{n}'_{DC} = \frac{4}{3\pi} n'_l \sigma_T c \alpha \frac{\langle h^2 \nu'^2 \rangle}{m_e c^2} n'_r \Lambda_{DC}, \tag{6}$$

where n'_r is the photon number density, $\Lambda_{DC} = \ln\left(\frac{KT'_s}{h\nu_{min}}\right) \bar{g}_{DC}$, and $\bar{g}_{DC}$ is a numerical factor which replaces the gaunt factor. We stress that the

photons within the transition region may not be in local equilibrium with the electrons (e.g. Blandford & Payne, 1981b; Riffert, 1988); nevertheless, Chluba et al. (2007) showed that if the average photon energy exceeds that of the electrons, the emission efficiency is reduced. Consequently, eq. (6) can be used as an upper limit.

Last, diffusion from the downstream provides an additional source of photons to the shock transition region. Downstream of x_s the photon number density continues to rise due to emission processes, until the photons regain thermodynamic equilibrium with the plasma. This leads to propagation of photons backward toward the upstream in a manner which can be treated as a diffusive process as long as $\dot{n}'_r/n'_r << (\sigma_T n'_{l,d}\beta_d c)$. The distance, L_D, which photons can cover by diffusion against the flow before being swept back, can be estimated by maximizing the expression $L_D = l_D - \beta_d ct$, where $l_D \equiv 2\sqrt{Dt}$ is the diffusion length and $D = \frac{c}{3n'_l\sigma_T}$ is the diffusion coefficient (e.g. Weaver, 1976, BP81a). This gives $L_D = \frac{1}{3n'_{l,d}\sigma_T\beta_d}$, implying that photons can diffuse back as long as $\beta_d < 1/3$, which always holds in a shock downstream. The total number density of photons at point x_s can thus be estimated by summing the total number of photons swept from the upstream with those which diffuse back from the downstream.

$$n'_{r,s} = \frac{n'_{r,u}u_u}{u_d}\left(1 + \frac{\int_{x_s-L_s}^{x_s+L_D}\dot{n}'_r dx}{n'_{r,u}u_u}\right) \equiv \frac{n'_{r,u}u_u}{u_d}\left(1+\zeta\right), \tag{7}$$

where $\dot{n}'_r \equiv \dot{n}'_{ff} + \dot{n}'_{DC}$. The dimensionless parameter ζ quantifies the relative contribution of photon production inside the shock and at the immediate downstream. Specifically, $\zeta \ll 1$ implies that the net production rate is much smaller than the incoming flux of photons, so that the radiation field in the shock transition is dominated by photons advected from the upstream. The upstream in this case is defined to be photon-rich. Relativistic temperatures or the presence of sufficient amount of pairs introduce additional emission processes such as pair creation and annihilation and e_+e_- Bremsstrahlung. However, as shown below, our analysis is restricted to situations where pairs are unimportant and temperatures are well below $m_e c^2$, therefore this possibility is ignored.

An upper limit on ζ can be derived analytically using the following assumptions:

1. Within the shock transition the photon flux is conserved to a good

approximation, i.e. $n'_{r,u}u_u = n'_{r,d}u_d$ and

$$KT'_s = P'_{r,d}u_d/n'_{r,u}u_u. \tag{8}$$

2. The photon production rate at the shock transition and the immediate downstream is constant and equals to the peak production rate of the shock at x_s.

3. The photons at x_s have a Wien distribution with a temperature that is equal to that of the electrons. In this limit $\langle h^2\nu'^2_s\rangle = 12\left(KT'_s\right)^2$.

The upper limit of ζ resulting from these assumptions is:

$$\zeta_c = \frac{n'_{l,d}\alpha}{n'_{l,u}\gamma_u\beta_u^2}\left(0.02\lambda_c^3 n'_{b,d}\Theta'^{-3}_u\Theta'^{-0.5}_s\Lambda_{ff} + 7\Theta'^2_s\frac{n_{r,d}}{n_{r,u}}\Lambda_{DC}\right), \tag{9}$$

where $\Theta' \equiv \frac{KT'}{m_ec^2}$. As it is shown below each term in the brackets becomes important at different regimes of upstream conditions. The first term is generally more important in the non relativistic limit, while the second term becomes important when the upstream has relativistic velocities.

In the limit where emission processes are negligible, the photon spectrum in the shock transition and in the immediate downstream is determined by a combination of thermal and bulk Comptonization. When thermal Comptonization is the dominant process, the photons establish a kinetic equilibrium with the electrons, resulting in a Wien spectrum. A hard non-thermal tail may evolve only when photons are upscattered by the bulk motion of the fluid at the upstream, and cross the shock before being thermalized. For a population of electrons with a non-relativistic temperature, the photon thermalization time is $t_T \sim \left(n'_b\sigma_T c\frac{4KT'_s}{m_ec^2}\right)^{-1}$. The shock crossing time is estimated differently for non-relativistic and relativistic upstreams, where in the non-relativistic case $t_s \sim \left(3n'_b\sigma_T c/\beta_u^2\right)^{-1}$. If however the upstream is relativistic $t_s \sim \left(n'_b\sigma_T c\tau/\gamma_u^2\right)^{-1}$, where τ is the optical depth of the shock transition for a photon coming from the *downstream*. LB08 calculated τ to be of the order of a few ($\tau \sim 3-5$), implying that a mutual parameter for both cases can be defined, $\Upsilon \equiv \frac{t_s}{t_T} \sim 12\frac{KT'_s}{m_ec^2}\frac{1}{\gamma_u^2\beta_u^2}$. If $\Upsilon < 1$, a photon that is upscattered at the upstream can cross the shock without loosing its energy to thermal scattering, and a high energy tail may evolve. Numerical simulations we preformed show that in the limit of $\Upsilon \to 0$, this tail is hard and reaches energies up to $\gamma_u m_ec^2$ in the shock frame (see §5).

4.1 Limits on the upstream conditions

In order to analyze the conditions under which the shock upstream can be considered photon-rich, we express the downstream quantities in eq.(9) in terms of the upstream values. Those are derived from the fluid equations, assuming conservation of total mass, energy and momentum across the shock. When $\beta_u \ll 1$ the shock jump conditions can be written as:

$$n'_{b,u}\beta_u = n'_{b,d}\beta_d, \tag{10}$$

$$\left(n'_{b,u}m_b c^2\frac{\beta_u^2}{2} + \frac{4}{3}P'_{r,u}\right)\beta_u = \left(n'_{b,d}m_p c^2\frac{\beta_d^2}{2} + \frac{4}{3}P'_{r,d}\right)\beta_d, \tag{11}$$

$$n'_{b,u}m_p c^2\beta_u^2 + P'_{r,u} = n'_{b,d}m_p c^2\beta_d^2 + P'_{r,d}, \tag{12}$$

Here we assume that at the upstream and downstream the contribution of baryon pressure is negligible. Such assumption is easily justified in photon-rich upstreams, since the number density of photons far exceeds that of the electrons and protons. In terms of the upstream parameters we therefore get:

$$\beta_d = \frac{\beta_u}{7}\left(1 + 8\frac{P'_{r,u}}{n'_{b,u}m_p c^2\beta_u^2}\right), \tag{13}$$

$$P'_{r,d} = \frac{6}{7}n'_{b,u}m_p c^2\beta_u^2\left(1 - \frac{1}{6}\frac{P'_{r,u}}{n'_{b,u}m_p c^2\beta_u^2}\right). \tag{14}$$

Note that the radiation pressure in the upstream is limited by $P'_{r,u} < \frac{3}{4}n'_{b,u}m_p c^2\beta_u^2$. Above this limit β_u is below the soundspeed, and no shock can form. We now substitute $P'_{r,u}$ and $n'_{b,u}$ with the dimensionless parameters $\tilde{P} \equiv \frac{P'_{r,u}}{n'_{b,u}m_p c^2}$ and $\tilde{N} \equiv \frac{n'_{r,u}}{n'_{b,u}}$, which relate to the original upstream parameters through:

$$KT'_u \simeq 90\ eV\ \tilde{P}_{-3}\tilde{N}_4^{-1}, \tag{15}$$

$$n'_{b,u} \simeq 2.4\times10^{15}\ cm^{-3}\ \tilde{P}_{-3}^3\tilde{N}_4^{-4}. \tag{16}$$

The resulting shock characteristic temperature in the non-relativistic limit is:

$$KT'_{s,NR} = 0.2\ KeV\ \tilde{N}_4^{-1}\beta_{-1}^2\frac{1 + 0.8\tilde{P}_{-3}\beta_{-1}^{-2}}{1.8} \tag{17}$$

and consequently, the derived upper limit for the relative number of newly created photons within the shock is:

$$\zeta_{NR} = 0.7\tilde{N}_4^{-0.5}\beta_{-1}^{-3}\Lambda_{ff,1}\left(\frac{1+0.8\tilde{P}_{-3}\beta_{-1}^{-2}}{1.8}\right)^{-2.5} + 1.2\times10^{-4}\tilde{N}_4^{-2}\beta_{-1}^{2}\Lambda_{DC,1}. \tag{18}$$

Since both parameters are defined in terms of the upstream values we dropped the subscript u for convenience.

When $\gamma_u\beta_u > 1$, T_s' and ζ_c can be estimated by solving the relativistic generalization of eqn. (10-12) and taking $\beta_d \sim 1/3$. This gives:

$$KT_{s,R}' \simeq 23\ KeV\ \tilde{N}_5^{-1}\gamma_1\left(1+0.04\tilde{P}_{-2}\right), \tag{19}$$

and

$$\zeta_R \simeq 0.1\tilde{N}_5^{-2}\gamma_1^3\Lambda_{DC,1}\left(1+0.04\tilde{P}_{-2}\right)^{-2}\left[1+0.04\frac{\tilde{N}_5^{1.5}}{\gamma_1^{2.5}}\frac{\Lambda_{ff,1}}{\Lambda_{DC,1}}\left(1+0.04\tilde{P}_{-2}\right)^{1.5}\right]. \tag{20}$$

The numerically calculated values of T_s' and ζ_c as a function of $\gamma_u\beta_u$, $\tilde{N}$ and $\tilde{P}$ are plotted in Fig (2). The figure is divided into 6 panels which represent different cuts in the $\tilde{N}-\tilde{P}$ plane. The left hand panels show plots made with $\tilde{P}=10^{-3},10^{-1},10$. In the right hand panels we fixed $\tilde{N}$ to be $\tilde{N}=10^3,10^4,10^5$ from top to bottom respectively. The orange lines are contours of equal T_s' in units of $\log_{10}\left(\frac{KT_s'}{eV}\right)$, whereas the light blue lines represent contours of equal ζ_c, with values $\zeta_c=0.1,1,10$. Below the black line the upstream Mach number <1, and no shock occurs. The region where photon advection from the upstream prevails in the shock transition is highlighted in gray, and is bounded by $\zeta_c=1$ and $KT_s' \lesssim 0.1 m_e c^2$. At this temperature the energetic photons in the tail of a Wien distributed radiation constitute $\lesssim 1\%$ of the total photons number, and their effect may be ignored. The real energy distribution may also include a non thermal energetic tail, where is such a case KT_s' represents the average photon energy rather than the Wien peak. This may affect the result, especially in the high $\gamma_u\beta_u$ regime (see §5). The green line describes constant values of $log_{10}(\Upsilon)$, where values <0 imply that the photons don't have time to reach thermal equilibrium with the electrons in the shock transition, and a high energy tail evolves. This allows for the generation of a high energy tail in the immediate downstream.

It can be seen that there is a considerable regime of parameters that result in RMS with photon-rich upstreams which are expected to develop prominent non-thermal tails.

4.2 Applications to GRB jets

Shocks may form in GRB jets due to various reasons, such as collision between converging flows (e.g. Levinson & Eichler, 2000; Bromberg & Levinson, 2007); interaction of the jet head with a stellar envelope of a collapsar, prior to its breakout (e.g. Matzner, 2003; Bromberg et al., 2011); or collisions of consecutive relativistic shells. But no matter the source of the dissipation, if it occurs below the photosphere it will form a RMS. Here we use the results obtained above to show that these shocks will most likely have photon-rich upstreams, and generate photon spectra with relatively low thermal peaks. Specifically in the case of shell collisions, the upstream velocity is mildly relativistic and the spectrum is expected to have a hard non-thermal tail.

Suppose that a shock is formed at some optical depth, τ, below the photosphere of a fireball, such as the one discussed in §3. The shock upstream condition is determined by the properties of the fireball at the corresponding dissipation radius. We can therefore use eq. (2) to calculate the flow parameters, $\tilde{N}$ and $\tilde{P}$ at that radius giving:

$$\tilde{N}_\tau = 1.25\times10^5 R_6^{1/4}\frac{\eta}{\eta_c}\Gamma_0^{-1/4}, \tag{21}$$

$$\tilde{P}_\tau = \frac{\tau^{1/3}}{4}\left(\frac{\eta}{\eta_c}\right)^{4/3}\begin{cases}\left[3-2\left(\frac{\eta_c}{\eta}\right)^4\right]^{1/3} & \tilde{\eta}_c<\tilde{\eta}\ll\eta_\pm,\\ \tau^{1/3}\left(\frac{\tilde{\eta}}{\tilde{\eta}_c}\right)^{4/3} & \tilde{\eta}<\tilde{\eta}_c.\end{cases} \tag{22}$$

By placing these expressions in eqn. (17)-(20) we can extract limits on the values of η which render the shock upstream photon-rich at that optical depth. In case where the shock has relativistic upstream, we get:

$$660L_{52}^{1/4}R_6^{-1/2}\gamma_{u,1}\Gamma_0^{1/2}\lesssim\eta\lesssim1.2\times10^4L_{52}^{1/4}R_6^{1/2}\gamma_{u,1}^{-3}\Gamma_0^{1/2}\tau^{-1}. \tag{23}$$

Below and above this regime the temperature at the immediate downstream exceeds $\sim 50\ KeV$ which we set as the limit above which and pairs may affect the flow. In the non relativistic limit shocks can form only if $\tilde{P}<0.75\beta_u^2$, corresponding to an upper limit of

$$\eta\lesssim480L_{52}^{1/4}R_6^{-1/4}\beta_{u,-1}^{3/4}\tau^{-1/4}, \tag{24}$$

where the lower limit should be derived numerically. Fig.(3) depicts the numerically calculated region for $\zeta_c < 1$ in the $\gamma_u \beta_u$ vs. η/η_c plane. Here we put $\tau = 1$ and $\Gamma_0 = 1$ for illustration. The color codes are similar to fig.(2).

In the standard internal shocks model where shocks from from shell collisions, τ and η are related via Eq. (3). The requirement that the shocks form below the photosphere restricts the jet's baryon load to $\eta < \eta_{ph}$, defined in eq. (4). This sets limits on $\tilde{N}$ and $\tilde{P}$, where taking $10^2\eta_2 < \eta < \eta_{ph}$ gives:

$$6.9{\cdot}10^3 L_{52}^{-1/4} R_6^{1/2} \eta_2 \Gamma_0^{-1/2} < \tilde{N}_{grb} < 2.5{\cdot}10^4 \left(\frac{b^2-1}{b^2}\frac{R_0}{c\delta t}\right)^{1/5} L_{52}^{-1/20} R_6^{3/10} \Gamma_0^{-1/2}, \tag{25}$$

and

$$3.1{\cdot}10^{-3} \left(\frac{b^2-1}{b^2}\frac{R_0}{c\delta t}\right)^{8/15} L_{52}^{-2/15} R_6^{2/15} < \tilde{P}_{grb} < 7.3{\cdot}10^{-3} \left(\frac{b^2-1}{b^2}\frac{R_0}{c\delta t}\right)^{2/3} \eta_2^{-2/3}, \tag{26}$$

where $b = \Gamma_2/\Gamma_1$ is the ratio between the Lorenz factors of the colliding shells, and $\Gamma_1 = \eta$. If we further assume that the shells have roughly the same mass, we can parameterize the upstream Lorenz factor at the shock frame. Equal mass shells have a center of mass which moves with a Lorenz factor $\Gamma_{CM} = \Gamma_1\sqrt{b}$. Consequently the Lorenz factor of each shell relative to the central mass is $\Gamma_{1,CM} = \Gamma_1\Gamma_{CM}\left(1-\beta_1\beta_{CM}\right) = \frac{1+b}{2\sqrt{b}}$, which for $b > 1$ gives an upstream Lorentz factor at the shock frame

$$\gamma_u \lesssim \sqrt{2}\Gamma_{1,CM} = \frac{1+b}{\sqrt{2b}}. \tag{27}$$

Placing these constraints in eq. (20) gives

$$6\cdot 10^{-4} L_{52}^{1/10} R_6^{-3/5} \Gamma_0 b^{3/2} \left(\frac{R_0}{c\Delta t}\right)^{2/5} \lesssim \zeta_c \lesssim 0.01 L_{52}^{1/2} R_6^{-1} \eta_2^{-2} \Gamma_0 b^{3/2}, \tag{28}$$

which imply that the shock transition is dominated by the upstream photons, and its temperature, derived from eq.(19) is:

$$6.5KeV\ L_{52}^{1/20} R_6^{-3/10} \sqrt{\Gamma_0 b} \left(\frac{c\Delta t}{R_0}\right)^{1/5} \lesssim KT_s' \lesssim 23KeV\ L_{52}^{1/4} R_6^{-1/2} \eta_2^{-1} \sqrt{\Gamma_0 b}. \tag{29}$$

At such a temperature $\Upsilon \ll 1$, and therefore a hard non-thermal tail may grow beyond the thermal peak. Such radiation-mediated internal shocks are

therefore expected to exhibit an observed thermal peak at energies of the order of a few MeV, together with a prominent hard non-thermal tail which may extend to a few hundreds MeV, depending on the optical depth at the shock location. A similar spectrum was observed in the initial phase of GRB 090902B.

5 Bulk Comptonization: Test particle MC simulations

To illustrate some basic properties of the spectral energy distribution of RRMSs with photon rich upstreams, we have preformed a 2D test particle Monte Carlo simulations, using the shock profiles computed self-consistently by LB08. For convenience, an analytic fit to these profiles was adopted,

$$U(\xi) = 0.5\,[\tanh(\alpha\xi) - 1]\,[U_d - U_u] + U_d. \tag{30}$$

where U_u is the far upstream 4-velocity, U_d is the far downstream 4-velocity and α is a free parameter that determines the width of the transition layer. The dimensionless variable ξ is related to the angle averaged optical depth across the shock. In terms of the coordinate x it is expressed as

$$\xi = n_u \sigma_T x, \tag{31}$$

where n_u is proper density far upstream and σ_T is the Thomson cross section. As stated above, these global shock solutions ignores KN effects and pair productions, and are suitable in the regime where convection of seed photons by the upstream flow is sufficiently large. As will be shown below, the neglect of pair production may not be justified at all for large enough upstream Lorentz factors. We have kept the full KN cross section in our test particle MC simulations to examine its effect on the spectrum, but ignored the thermal spread of the electrons in the shock and downstream. Thus, the results are relevant for photons above the thermal peak.

The injected photons are drawn from a monochromatic and isotropic (in the fluid rest frame) source of photons, located at a fixed position within the simulation box, as viewed in the shock frame. We have run simulations for different source locations, including injection from the immediate upstream and immediate downstream, and found little differences in the resultant spectrum as long as the optical depth from the injection point to the

shock transition is not too large. The boundaries of the simulation box are defined by two values of the variable ξ, ξ_{min} and ξ_{max}, where ξ_{min} is located upstream and ξ_{max} downstream. The boundaries ξ_{min} and ξ_{max} are chosen to optimize the run time without affecting the resultant spectrum. That is, it has to be large enough to allow injected photons to undergo the maximum number of scattering across the shock, but minimum number of scattering in the far downstream, where the probability to recross the shock becomes very small. The location of ξ_{min} is chosen such that less then 2% of the injected photons escape the simulation box though the upstream boundary.

For each of the results presented in Figs. (4) and (5) below 10^7 photons were injected in the immediate downstream. The trajectory of each photon was followed until it "escaped" the simulation box from either side. Fig. (4) delineates the effect of the upstream Lorentz factor on the spectrum at the immediate downstream. The width of the shocks in both cases is $\tau = 3$, which roughly gives the profile computed in LB08, where τ is the Thomson depth for a photon moving from the downstream, at $U(\xi_d) = U_d(1 + 10^{-4})$, to the point $U(\xi_u) = 0.9U_u$ upstream, viz.,

$$\tau = \int_{\xi_u}^{\xi_d} \gamma(\xi)(1+\beta)d\xi, \tag{32}$$

with $\gamma(\xi) = [U^2(\xi) + 1]^{1/2}$ and $\beta = U/\gamma$ for the profile given in Eq. 30. As seen, the spectrum hardens with increasing Lorentz factor, but even for modest ones we find that a considerable fraction of the shock energy is transferred to photons near the KN limit. The effect of the shock width on the photon spectrum is explored in Fig. 5. We have also performed runs for different injection points, including photon injection upstream, and found only small differences in the resulted spectra. We conclude that the location where photons are injected does not affect the spectrum considerably.

In all cases studied a hard spectrum was obtained, extending over several decades in energy. For sufficiently high injection energies the statistics allowed us to follow the spectrum up to the KN limit, $\gamma_u m_e c^2$, as measured in the shock frame. There is no evidence for a cutoff or steepening at energies well below the KN limit, in any of the experiments performed. As naively expected, the spectrum is somewhat harder for larger upstream Lorentz factors. There is also a weak dependence on the shock width. The profiles computed in LB08 are relatively narrow, in the sense that the angle averaged optical depth of the order of a few ($\tau \sim 3 - 5$). As demonstrated by

Budnik et al. (2010), pair production upstream can lead to a photon breading cycle that can boost the upper cutoff well above the KN limit, up to an energy of $\gamma_u^2 m_e c^2$ in case of sufficiently relativistic shocks. The temperature in the immediate downstream in the case of photon rich upstream is much smaller than in the case of a cold upstream studied by Budnik et al. (2010). Nevertheless our test particle simulations illustrate that pair production by the accelerated photons is expected to be important, especially in the case of moderate to high upstream Lorenz factor, and might alter the details of the resultant spectrum.

6 Conclusions

In this paper we consider sub-photospheric emission by relativistic radiation mediated shocks in the prompt phase of GRBs. The main conclusions are:

1. Dissipation via internal shocks is likely to occur over a range of radii that encompasses the photosphere. Slower shells should collide below the photosphere, at a moderate optical depth (unless the time separation between consecutive ejections is much larger than the dynamical time of the engine), whereas shells ejected with sufficiently large Lorentz factor will collide above the photosphere. The fraction of the energy that dissipates below the photosphere depends on the burst parameters, and may significantly vary from burst to burst. Specific examples, for which measurements of the luminosity and estimates of the Lorentz factors are available were analyzed. In case of GRB 090902B we conclude that a major fraction of the explosion energy dissipated below the photosphere, in a region of optical depths < 300, via relativistic radiation mediated shocks. For GRB 080916C we find that collision of shells occurred predominantly above the photosphere, giving rise to formation of collisionless shocks.

2. Shocks that form below the photosphere are mediated by Compton scattering of radiation produced inside the shock or advected by the upstream flow. Since the scale of the shock, a few Thomson lengths, is vastly larger than any kinetic scale involved, particle acceleration by the Fermi process is highly unlikely in such shocks. On the other hand, bulk Comptonization gives rise to a hard spectrum extending above a (thermal) Wien peak, up to the KN limit $\gamma_u m_e c^2$ (and perhaps beyond, e.g., Budnik et al. 2010), where γ_u is the Lorentz factor of the upstream flow, measured in the shock frame. The mean photon energy in the immediate downstream is determined by the

number of photons advected into and/or produced inside the shock. For a cold upstream, a condition expected in shock breakout episodes, the Wien temperature is $\sim m_e c^2$ (Budnik et al. 2010). However, under the conditions anticipated in the prompt phase of GRBs, the shock upstream is photon rich, in the sense that photon advection largely dominates over photon production, and the thermal peak is located at energies well below $m_e c^2$. We estimate temperatures in the range between a few and a few tens keV for typical GRB parameters.

The existence of the hard spectral component is demonstrated in this work through test particle Monte Carlo simulations on given shock profiles, that were computed in an earlier work (Levinson and Bromberg 2008), neglecting pair production by MeV photons and the thermal spread of the electrons. The resultant spectra extend to the KN limit, which imply that pair production inside the shock is likely to be important in photon rich shocks. A full treatment requires a proper account of this process in the computation of the shock structure and the resultant spectrum.

Acknowledgments

We thank Ehud Nakar and Re'em Sari for enlightening discussions. This research was supported by an ERC advanced research grant, and by by an ISF grant for the Israeli center for high energy astrophysics.

References

Abdo A. A., et al., 2009a, Sci, 323, 1688

Abdo A. A., et al., 2009b, ApJ, 706, L138

Ackermann M., et al., 2010, ApJ, 716, 1178

Band D., et al., 1993, ApJ, 413, 281

Becker P. A., 1988, ApJ, 327, 772

Blandford R., & Eichler D., 1987, PhR, 154, 1

Blandford R. D., & Payne D. G., 1981a, MNRAS, 194, 1041; BP81a

Blandford R. D., & Payne D. G., 1981b, MNRAS, 194, 1033; BP81b

Blandford R. D., & Payne D. G., 1981c, MNRAS, 196, 781

Bromberg O., & Levinson A., 2007, ApJ, 671, 678; BL07

Bromberg O., et al., 2011, in prep.

Budnik R., Katz B., Sagiv A., Waxman E., 2010, ApJ, 725, 63

Colgate S. A., & Chen Y.-H., 1972, Ap&SS, 17, 325

Chluba J., Sazonov S. Y., & Sunyaev R. A., 2007, A&A, 468, 785

Eichler, D. 1994, Astrophys. J. Supp., 90, 877

Eichler, D., & Levinson, A. 2000, ApJ, 529, 146

Hsieh S. H. & Spiegel E. A., 1976, ApJ, 207, 244

Katz B., Budnik R., Waxman E., 2010, ApJ, 716, 781

Laurent P. & Titarchuk L. G., 2001, Astrophys. J. Lett., 562, L67

Levinson A., & Bromberg O., 2008, PhRvL, 100, 131101

Levinson A., Eichler D., 1993, ApJ, 418, 386

Levinson A., Eichler D., 2000, PhRvL, 85, 236

Lyubarsky Y., & Sunyaev R. A., 1982, Soviet Astron. Lett, 8, 330

Matzner C. D., 2003, MNRAS, 345, 575

Matzner C. D., & McKee C. F., 1999, ApJ, 510, 379

Mészáros P., Laguna P., Rees M. J., 1993, ApJ, 415, 181

Mészáros P., & Rees M. J., 2000, ApJ, 530, 292

Mészáros P., & Waxman E., Phys. Rev. Lett. **87**, 171102 (2001)

Nakar E., Piran T., & Sari R., 2005, ApJ, 635, 516

Pai S. I., 1966, in "Radiation gas dynamics, Springer-Verlag" New York, NY, 1966.

Paczynski B., 1990, ApJ, 363, 218

Pelassa V., Ohno M., 2010, arXiv, arXiv:1002.2863

Rees M. J., Meszaros P., 1994, ApJ, 430, L93

Riffert, H., ApJ, 327, 760 (1988)

Rybicki G. B., Lightman A. P., 1979, in "Radiative Processes in Astrophysics", New York, NY, 1979.

Ryde F., 2005, ApJ, 625, L95

Ryde F., et al., 2010, ApJ, 709, L172

Sari R., Piran T., 1997, MNRAS, 287, 110

Shemi A., Piran T., 1990, ApJ, 365, L55

Spitzer L., 1978, in "Physical processes in the interstellar medium", New York Wiley-Interscience, 1978.

Svensson R., 1984, MNRAS, 209, 175

Titarchuk L. G., 1997, ApJ 487, 834

Weaver T.A., 1976, Astrophys. J. Supp., 32, 233

Zel'dovich, Ya. B. & Raizer, Yu. P., 1967, in "Physics of Shock Waves and High-Temperature Hydrodynamic Phenomena" , Academic Press, New York, 1967

Zou Y.-C., Fan Y.-Z., Piran T., 2011, ApJ, 726, L2

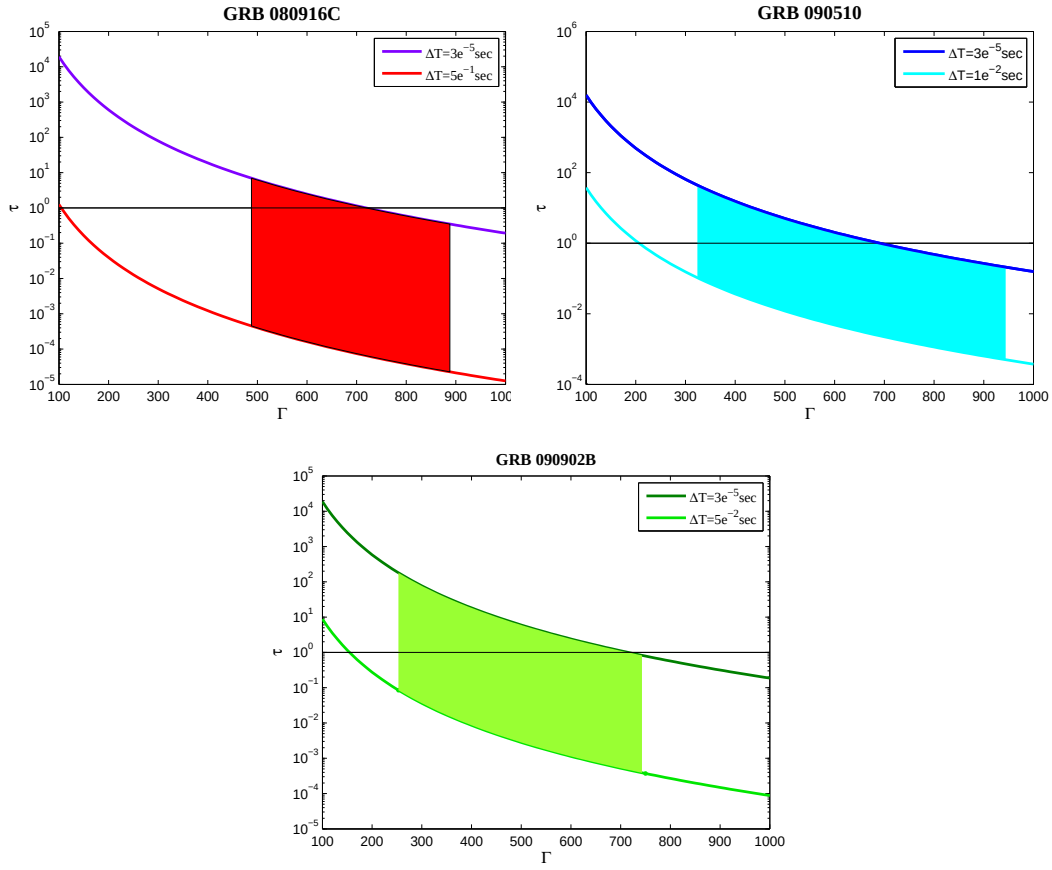

Figure 1 The optical depth at the shock location calculated for different Lorentz factors and time separation of the ejected shells, in 3 Fermi GRBs. The curve lines depict constant δt, taken between a minimal dynamic time scale to a maximal value taken to be the observed variability by *Fermi* BGO detector. The colored areas show the range of Γ and δt relevant for each burst.

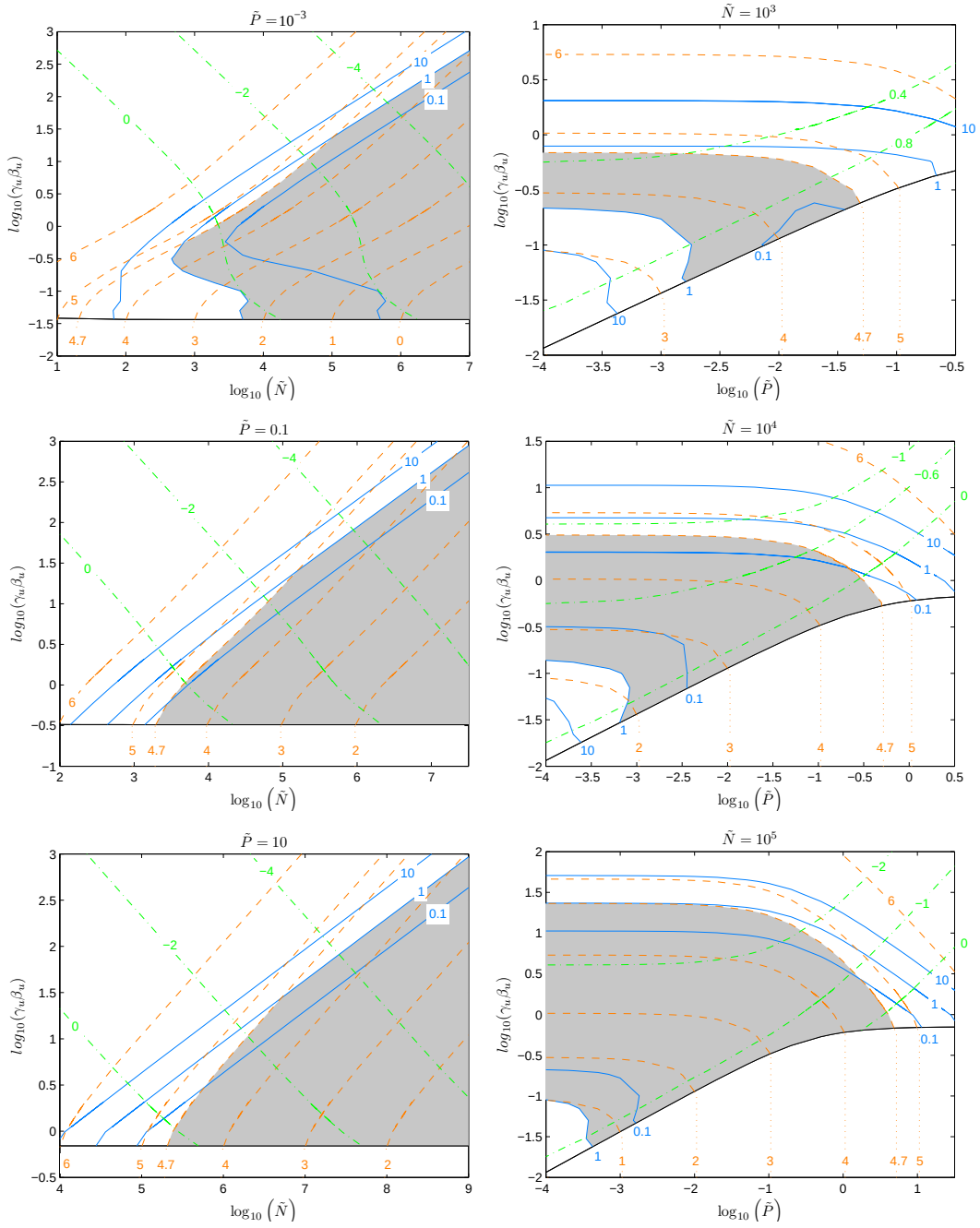

Figure 2 Contour lines of equal ζ_c (light blue) and $\log_{10}\left(\frac{KT'_s}{eV}\right)$ (orange), presented on a $\gamma_u\beta_u$ vs. $\tilde{N}$ (left panels) and $\tilde{P}$ (right panels). Areas marked in gray correspond those parts in the transition region where the advection of photons from the upstream dominates over emission processes, and the temperatures are NR. The green line depicts constant values of $log_{10}(\Upsilon)$, where values < 0 imply that a high energy spectral tail may evolve in the shock transition. Below the black line shocks can not form since the Mach number < 1.

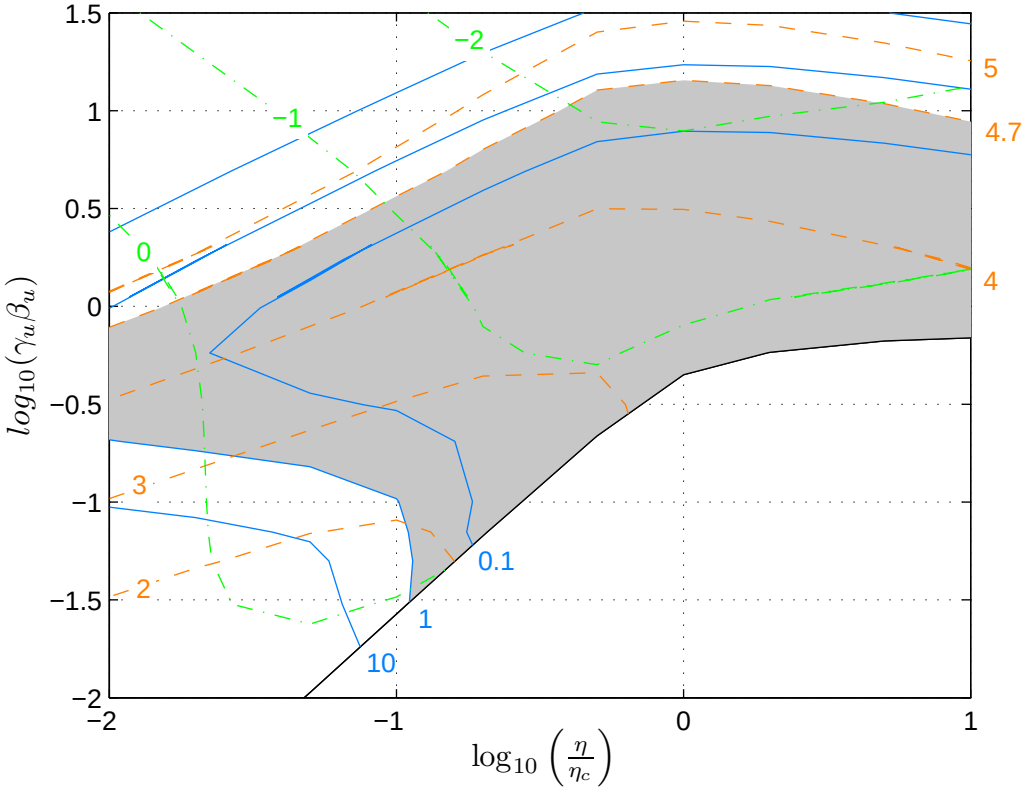

Figure 3 Contour lines of equal ζ_c (light blue) and $\log_{10}\left(\frac{KT'_s}{eV}\right)$ (orange), presented on a $\gamma_u\beta_u$ vs. η/η_c plane. The values here are calculated on the photosphere. Areas marked in gray correspond those parts in the transition region where the photons advection dominates over emission processes, and the temperatures are NR. The green line depicts constant values of $log_{10}(\Upsilon)$, where values < 0 imply that a high energy spectral tail may evolve in the shock transition. Below the black line shocks can not form since the Mach number < 1.

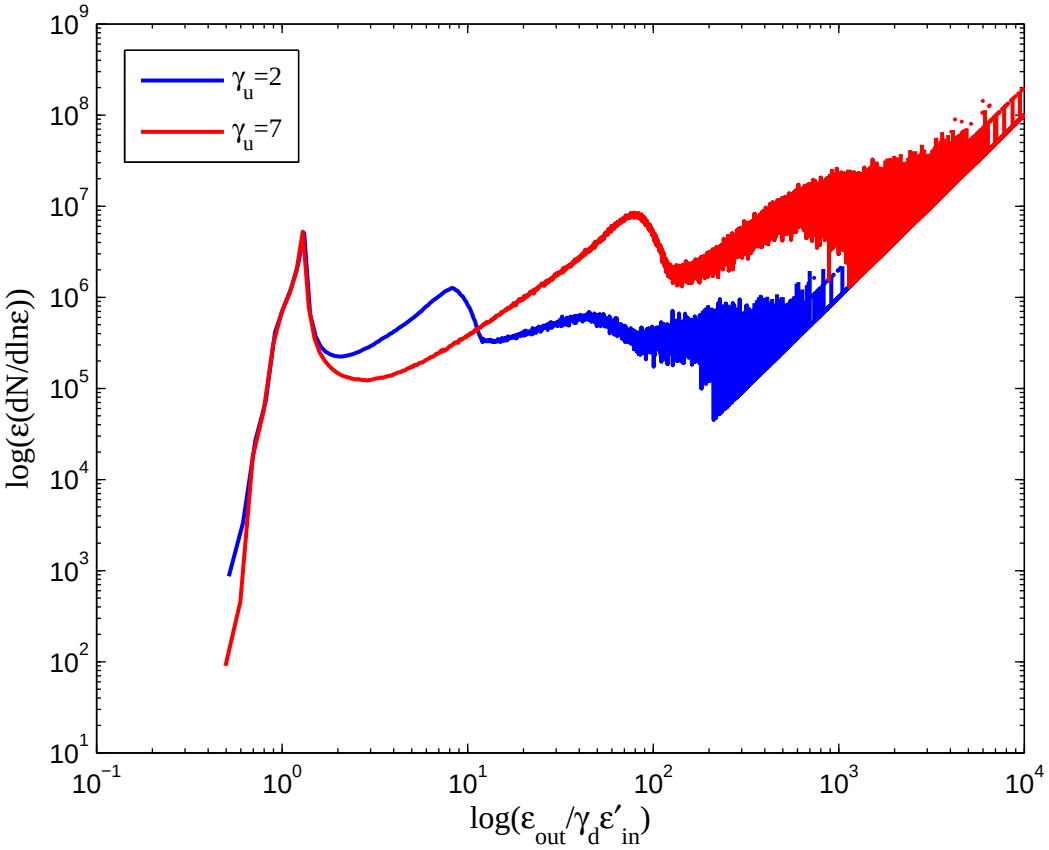

Figure 4 The angle averaged spectral energy distribution in the immediate downstream of a RRMS of width $\tau = 3$ and Lorentz factor $\gamma_u = 2$ (red) and $\gamma_u = 7$ (blue), as measured in the shock frame. The downstream velocity in both cases is taken to be $\beta_d = 1/3$. The calculated energy is normalized to the initial injection energy, $\gamma_d \epsilon'_{in}$, with $\epsilon'_{in} = 100$ ev in the fluid frame.

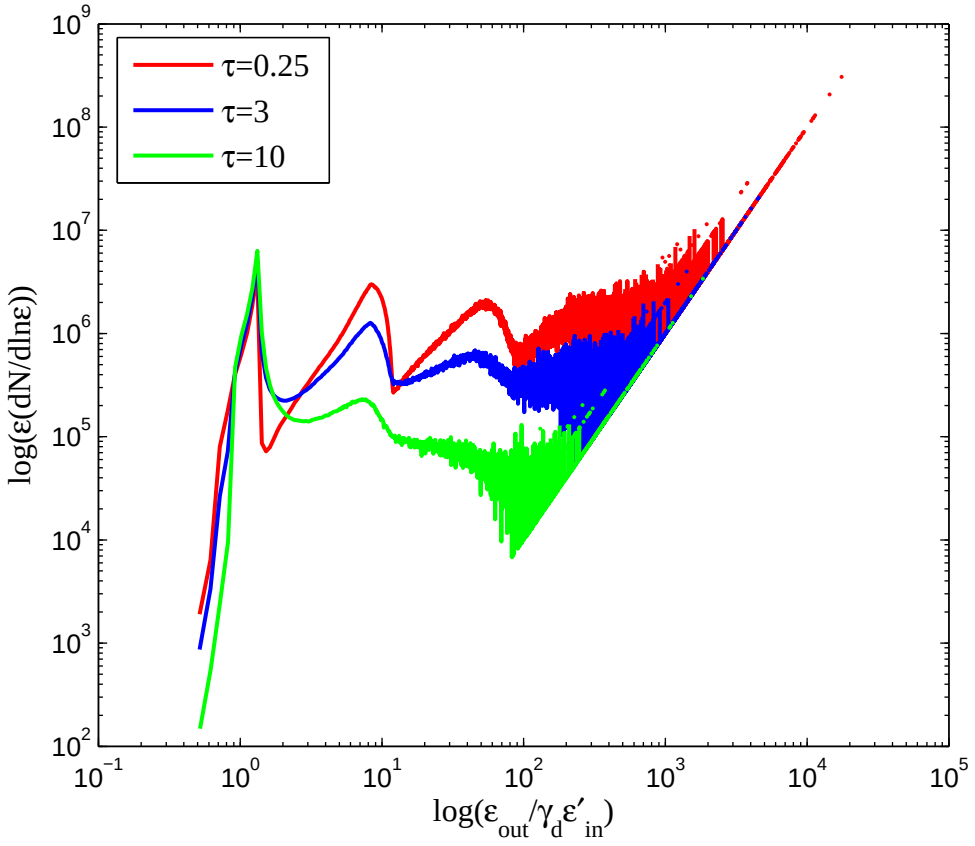

Figure 5 Same as Fig 4, but for an upstream Lorentz factor $\gamma_u = 2$ and different values of τ.